ESRF	**Experiment title:** In-situ surface x-ray diffraction studies of Cu(111) homoepitaxial electrodeposition in organic additive containing electrolyte	**Experiment number**: SI-2074
Beamline: ID 32	**Date of experiment**: from: 28/04/2010 to: 05/05/2010	**Date of report**: 28/11/2011
Shifts: 18	**Local contact(s)**: Parasmani Rajput	*Received at ESRF:*

Names and affiliations of applicants (* indicates experimentalists):

F. Golks*[2], Y. Gruender*[1], J. Stettner*[1], A. Drünkler*[1], O. M. Magnussen[1]

[1] Institut für Experimentelle und Angewandte Physik, Universität Kiel, Leibnizstr. 19, D-24089 Kiel, Germany
[2] European Synchrotron Radiation Facility, 6, Rue Jules Horowitz, F - 38000 Grenoble

Report:

Experiments were carried out at beamline ID32 (E_{Ph}= 22.5 keV) using a hanging meniscus transmission cell which proved to be well suited for in-situ surface x-ray diffraction studies of rapid structural changes at interfaces with simultaneous high quality electrochemical measurements. In order to have high time resolution, i.e. ~10 Hz, and the capability of recording entire peak profiles of rod cross sections in single shots, we used our one-dimensional detector (Dectris Mythen 1K, cp. SI-1999). From the peak profiles transients of integrated peak intensities and widths are obtained.

In the first part of the experiment we investigated the complex interplay of the chloride adlayer, specifically its disorder/order phase transition [1,2], and the Cu electroplating process in 0.1 M $HClO_4$ + 1 mM HCl + 1 mM $CuClO_4$. Since chloride is a standard component in today's industrially used plating baths [3], but its key role in the plating process is not yet understood on the atomic scale, these studies are of great importance. In continuation of our experiment SI-1999, we studied the system after initiation of the deposition process via exchange from Cu-free to Cu-containing electrolyte. In parallel to electrochemical experiments, in which the electrode potential was stepped from -0.6 V (vs. Ag/AgCl) to different E_{end}, the scattered intensity was first recorded on the superstructure rod [(1,0,0.1), sensitive to Cl c(2x2) coverage], then close to anti-Bragg position on the CTR [(1,1,0.1), related to the ordering state independent overall Cl coverage and substrate roughness/growth behaviour]. Thus, the Cl c(2x2) superstructure and its formation as well as the substrate morphology can be studied separately. Interesting details in the time-dependent integrated intensity transients are observable upon direct comparison of both transients at (1,0,0.1) and (1,1,0.1) for the appropriate potential step experiments. Fig. 1 (a) shows as an example the comparison for the potential step to E_{end} = -350 mV. The intensity at (1,1,0.1) shows layer-by-layer growth oscillations as already found in SI-1999 (black curve). The integrated intensity at (1,0,0.1) (red curve) increases with time until it reaches its saturation after approximately 30 seconds. At that time, the growth oscillations vanish and a subsequent constant intensity manifests the transition from layer-by-layer growth to step-flow growth [4]. The coincidence of both processes strongly suggests a mutual interplay of the c(2x2) Cl adlayer ordering and the growth behaviour. The analysis of the FWHM of the superstructure rod at (1,0,0.1), shown in figure 1 (b), supports this model as the decrease in FWHM from 0.037 to 0.030 degree indicates the formation of long range correlations of the ordered Cl terraces. After the transition to step-flow growth, the FWHM stays on a constant level. The initial overshoot in the integrated intensity as well as FWHM of the Cl rod can be explained by the fact that an

initially smooth surface roughens during the first ~ 3 s of deposition, i.e. the intensity and FWHM decrease and increases, respectively.

Second, we investigated the influence of the organic additive polyethylene glycol (PEG) on the atomic scale morphology of our system. As in the case of chloride, PEG is used as inhibitor in modern copper electroplating baths [3] with the aim of slowing down the plating process at curvature enhanced areas of the interface. Comparatively fast measurements of the interface structure after exchange to PEG-containing electrolyte were necessary in order to exclude beam influence effects on the system. Using the Mythen 1K detector, crystal truncation rod (CTR) measurements were performed for the non-specular rods (1,0), (1,1), (2,0) and the specular rod (0,0) within ~8 min (instead of ~2 hours with the Cyberstar point detector). CTRs were measured at -550 and -200 mV before and after the exchange to PEG-containing electrolyte. The direct comparison of the L-dependent square of the structure factor shows significant differences in case of the potential -550 mV, and here only for the (1,0), (1,1) and specular rods (figure 2). Noteworthy, the (1,0) superstructure rod exhibits a modulation in its L-dependence as previously observed by our group and recently published in [2].

Third, we investigated the structure and potential dependent compression effect of the electrodeposited chloride adlayer on Cu(111) in 0.1M NaClO$_4$ + 0.1 mM HCl. This work is published in Surface Science [5]:
Title: Structure and electrocompression of chloride adlayers on Cu(111).

Abstract: The specific adsorption of chloride on Cu(111) from acidic aqueous electrolyte (pH 3) was investigated by in-situ surface X-ray diffraction, revealing an incommensurate hexagonal rotated adlayer. The structure and its potential dependence suggest a strong adsorbate-adsorbate interaction as compared to other halide adlayers on (111)-oriented metal electrode surfaces. The orientational epitaxy can be rationalized by the model suggested by Grey and Bohr (Europhys. Lett. 18, 171, 1992), which is based on symmetry considerations.
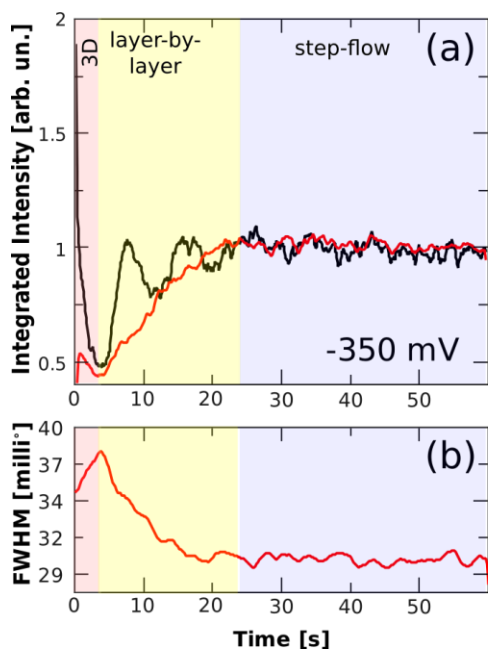
Fig. 1: (a) Time-dependent scattered intensity at (1,1,0.1) (black) and (1,0,0.1) (red) upon potential step from -0.6 V to E$_{end}$=-350 mV. The black curve exhibits layer-by-layer growth oscillations. The red curve is the integrated intensity at (1,0,0.1).
(b) Time-dependent FWHM of the Cl rod.
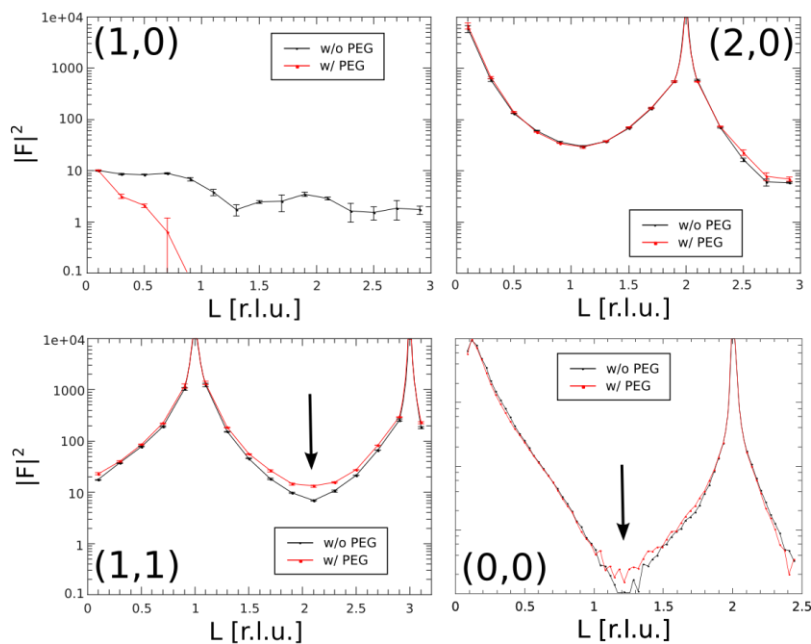
Fig. 2: Crystal truncation rod measurements of the (1,0), (2,0), (1,1) and (0,0) rod in absence (black curve) and presence (red curve) of PEG at -550 mV. The superstructure rod (1,0) exhibits significant modifications due to the presence of PEG. Further differences are observable in the (1,1) and (0,0) rod near anti Bragg (arrow).

References:

[1] M. Vogt, A. Lachenwitzer, O.M. Magnussen, R. Behm, Surf. Sci. 399 (1), 49–69 (1998)

[2] Y. Gründer, D. Kaminski, F. Golks, K. Krug, J. Stettner, O. M. Magnussen, A. Franke, J. Stremme, E. Pehlke, Phys. Rev. B, 81, 17 (2010)

[3] D. Josell, D. Wheeler, W.H. Huber, T.P. Moffat, Phys. Rev. Lett. 87, 016102-1 (2001)

[4] K. Krug, J. Stettner, O.M. Magnussen, Phys. Rev. Let. 96, 246101 (2006)

[5] Y. Gründer, A. Drünkler, F. Golks, G. Wijts, J. Stettner, J. Zegenhagen, O.M. Magnussen, Surf. Sci. 605, 1732-1737 (2011)